Proceedings of the ASME 2019
International Mechanical Engineering Congress and Exposition
IMECE2019
November 11-14, 2019, Salt Lake City, UT, USA

IMECE2019-10460

LOW-COST PARTICULATE DETECTION IN BLEED AIR

Mir Seliman Waez[1], Steven J. Eckels, Christopher M. Sorensen
Kansas State University
Manhattan, KS

ABSTRACT

Bleed air is brought into aircraft cabins in order to maintain the quality of the air for passenger and crew health and comfort. The bleed air can be contaminated by oil due to oil seal leaks in the compressor which have been reported randomly and generated significant public interest. Previous studies have measured the particulate size distribution in the bleed air entering the cabin, but never distinguished the type and material of the particulate matter (PM). The particulates could be potentially hazardous oil droplets from the oil seal leaks, water droplets due the presence of fog generated by the cooling system, and so on. In this study we propose a novel technique using light scattering technology to distinguish between contaminant types. This technique uses size and complex index of refraction as the measure. Since each material has a distinct index of refraction, by determining the index of refraction, our proposed low-cost detector could distinguish the compound in the aerosol as well as determine the particle size simultaneously.

Keywords: Particulate, Particle Size, Index of refraction, Bleed air, Light scattering

NOMENCLATURE

The following parameters/symbols are used in this paper:

$I(r)$	intensity as a function of radius
I_0	peak intensity at the center of the beam
r	radius of the beam
w	beam waist
P_{Tot}	total power in the beam
Θ	scattering angle
$\Delta\Omega$	solid angle
P_{scat}	scattered power on the photodiode
$dC/d\Omega$	differential scattering cross-section
V_i	output voltage of the photodiode at position i
$R(\lambda)$	responsivity of the photodiode
λ	wavelength
K	conversion factor of the photodiode
d_i	cord length
v	velocity of the particle
d_3	maximum length at the center of diamond
x_i	horizontal position along the beam radius
Ω_c	solid angle at the center of the beam
Ω_i	solid angle at any x_i position

1. INTRODUCTION

Bleed air is introduced in commercial aircraft cabins to provide ventilation air for the passengers and crew health and comfort. The most common method of conditioning aircraft cabins has been through the use of bleed air from the aircraft jet engine compressor [1]. However, the drawback for this method is that bleed air can be contaminated by lubricating oil due to bearing seal leakage or other fluids ingested into engine air intake, which is then introduced into the cabin as potentially hazardous oil mist. Health effects for passengers and crew during these incidents are diverse, ranging from eye and throat irritation and blurred vision to disorientation, nausea, vomiting, dizziness, or even loss of consciousness [2]. When the contamination is high, it creates fume event that shows an obvious odor or sometimes visible smoke or mist in the aircraft [3]. In the case of visible smoke, and if the source of the smoke is unidentified, the crew members may decide for an emergency landing.

To provide air representative of oil contaminated bleed air, a bleed air simulator was developed to show what would be expected in the case of aircraft cabin contamination [4]. To analyze and characterize the contaminants that would likely be present in the bleed air during an incident, multiple papers have been published identifying chemicals present in the oil and discussing their health risks and effects [5-7]. Moreover, volatile organic compounds (VOC) generated by the pyrolysis of the lubricating oil at high temperatures expected in the bleed air system have been studied and identified as well [8-10].

[1] Contact author: swaez@ksu.edu

While considerable work has been done to improve the air quality in aircraft cabins by identifying and characterizing the contaminants that would be present in the bleed air as mentioned above, real-time detecting, sizing, and distinguishing the type and material of single particles in bleed air is still missing from the bulk of research.

To determine the size and index of refraction, twin-angle optical particle counters (OPCs) that measured the scattered light at two angles, i.e., 40° and 74°; 60° and 90° were developed [11, 12]. These OPCs could measure the average refractive index and size distribution of aerosol particles. However, in order to distinguish the contaminant material in bleed air, it is important to measure the refractive index of each single particle as opposed to the average value of the refractive index.

In this study, we propose a novel technique using light scattering technology to distinguish between contaminant types. This technique uses size and complex index of refraction as the measure. Since each material has a distinct index of refraction, by determining the index of refraction, our proposed low-cost detector could distinguish the compound in the aerosol as well as determine the particle size simultaneously. Once the compound in the bleed air has been identified, considering its health effects to the passengers, it will help the cabin crew members get the right decision whether or not an emergency landing is required.

The majority of the optical particle detectors use laser as the light source. An important aspect of any optical detector is to know the incident intensity on the particle. Most light sources, a laser beam for example, have an intensity profile across the beam. For many laser sources, the profile is Gaussian. Thus the position of the particle in that profile must be known and controlled in order to accurately size the particle and distinguish its type and material. Most of the low-cost optical devices assume that the particles are passing through the center of the sensing volume, but the light scattered intensity of a particle can be significantly different if it passes through the very center or off-center which will lead to inaccurate determination of the size, type, and material of the particle. To control the precise position of the particle, and record the precise intensity, a diamond shaped beam aperture has been used to make a correction for the Gaussian beam [13]. In this paper, we have considered the same correction.

2. MATERIALS AND METHODS

A diamond-shaped beam aperture has been used to make a correction for the Gaussian intensity distribution of a typical laser [13] as shown in Figure 1.

With the diamond shape centered on the Gaussian profile, the time of fight of a particle through the beam is related to where the particle's path is positioned relative to the Gaussian center. Thus by measuring the time of flight, the incident intensity for the scattering is determined regardless of where the particle passes through the beam, and the particle can be sized accurately. In addition, it was shown that at an optimum scattering angle of 37°, particles can be sized independent of the real part of the refractive index; however, it still depends on the imaginary part. Photodiode positioned at ±37° scattering angle was used to record the scattered light intensity of the particle instantaneously for as long as the particle was inside the beam. Then total time of flight and scattered light-peak intensity were used to predict particle size.

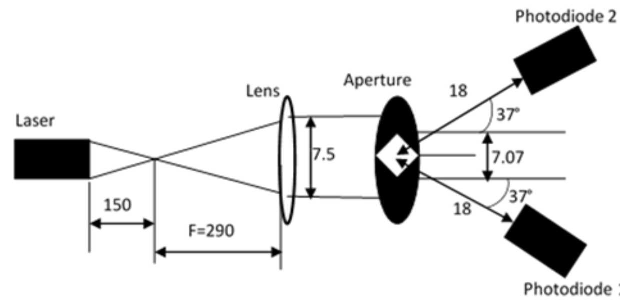

FIGURE 1: GAUSSIAN BEAM CORRECTION, DIMENSIONS (mm) [13]

Figure 2 shows the details of the diamond-shaped aperture.

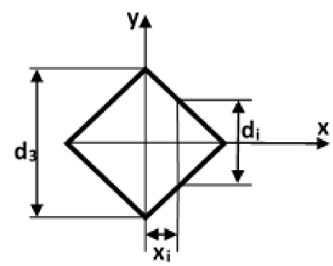

FIGURE 2: DIAMOND-SHAPED BEAM APERTURE [13]

In practical light-scattering systems, only a portion of the scattered light is gathered by a photodiode, which rests at a given angle. Such measurements are related to the differential scattering cross-section of the particle. The functional relationship of the differential scattering cross-section averaged over 10° range with scattering angle for different refractive indices is shown in Figure 3. In this figure we can see that at a scattering angle of 37±5°, the differential scattering cross-section shows relative independent of the real part of the refractive indices for 10 µm particles and above; however, as the particles get smaller, the independence gets reduced. Therefore, particles of 10 µm in diameter and above can be sized regardless of what their real refractive indices are. To determine the refractive index, it is instructive to detect the scattered light at a second angle where the differential scattering cross-section varies more consistently compared to the other angles. By measuring the scattered light intensity at two angles simultaneously, we can determine the two unknowns, i.e., particle diameter and the refractive index. For particle detection applications, the refractive index is not known ahead of time, but the particles being present in the bleed air would most likely be due to fog, engine oil, or lubricating oil with known refractive indices. Once our detector determines the refractive index, the type and material of the particulates in the bleed air can be identified as well.

2.1 Experimental Setup

The instantaneous scattered light intensity of single particles at ±37° scattering angle for the particles passing through a diamond-shaped beam is shown in Figure 1. The 37° can be used to only determine the particle size with no refractive index information. To determine the refractive index, we would like to propose that the light scattered intensity be detected simultaneously at 90° scattering angle which depends on both size and refractive index, as we can see in Figure 3.

To include the 90°, we have modified Figure 2 for our new experimental setup as we can see in Figure 4. The experimental setup uses a Laserglow BDG005XXX, 5-mW, 532-nm wavelength laser; a collimating lens; an aperture to make a diamond-shaped beam profile with dimensions of 5mm x 5mm; a focusing lens which focuses the diamond shaped beam; and two Thorlabs SM05PD1A photodiodes with a responsivity of R (532 nm) = 0.32 A/W positioned at 37° and 90° scattering angles. A Thorlabs PDA200C photodiode amplifier with a conversion coefficient of 1 x 10^7 V/A is used to display the scattered-light signal detected by the photodiodes. A National Instruments (NI) data acquisition system is connected to the photodiode amplifier and LabVIEW program to record the data. This experimental setup can be used to determine the size, and index of refraction of particles simultaneously.

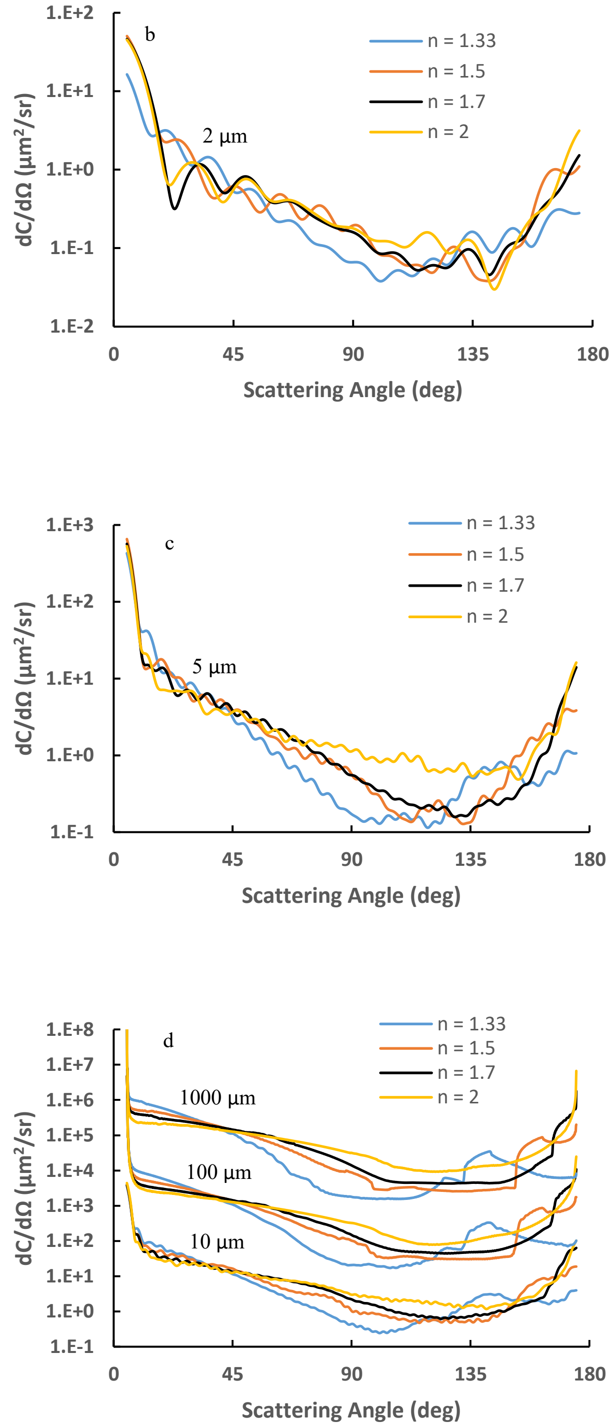

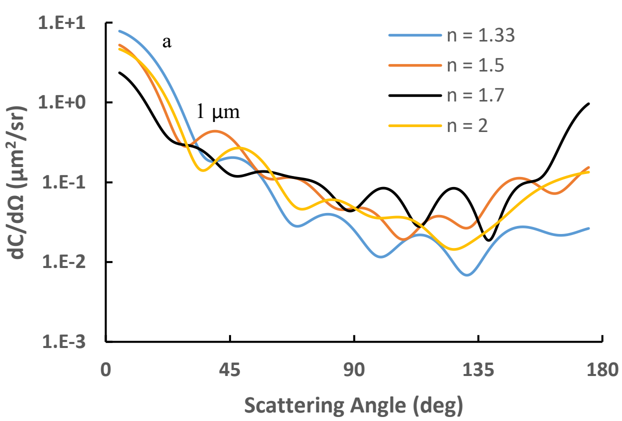

FIGURE 3: AVERAGE DIFFERENTIAL SCATTERING CROSS-SECTION OVER A 10° SCATTERING ANGLE FOR FOUR DIFFERENT REFRACTIVE INDICES AND DIFFERENT PARTICLE DIAMETERS, d (REPLOTTED [13])

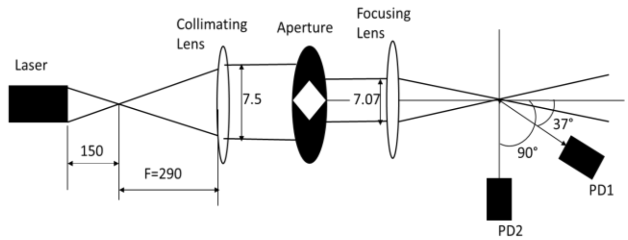

FIGURE 4: EXPERIMENTAL SETUP, DIMENSIONS (mm)

3. THEORETICAL ANALYSIS

A theoretical model has been developed to determine the particle diameter independent of the real part of the refractive index [13]. This model considers the Gaussian beam equation to relate the beam geometry to the parameters related to the laser, photodiode, photodiode amplifier and so on. For a Gaussian beam,

$$I(r) = I_0\, e^{-(2r^2/w^2)} \tag{1}$$

where $I(r)$ is the intensity as a function of the beam radius, I_0 is the peak intensity at the center of the beam, r is the radial distance from the beam center, and w is the beam waist. The radial distance in rectangular coordinates is

$$r = \sqrt{x^2 + y^2} \tag{2}$$

To find the total power in the beam, Eq. (1) can be integrated.

$$P_{Tot} = I_0 \int_0^{\infty} \int_0^{2\pi} e^{-(2r^2/w^2)} r dr d\theta = {}^{\pi}\!/_{2}\, I_0 w^2 \tag{3}$$

Since P_{Tot} is generally a known parameter, Eq. (3) can be solved for I_0. The scattered power on the photodiode can be found by multiplying Eq. (1) by the differential scattering cross-section and a solid angle, $\Delta\Omega$ that the photodiode makes with the particle position in the beam.

$$P_{scat} = I_0\, e^{-(2r^2/w^2)}\, {}^{dC}\!/_{d\Omega}\, \Delta\Omega \tag{4}$$

The output voltage of the photodiode can be obtained by

$$V_i = P_{scat} * R(\lambda) * K \tag{5}$$

Where $R(\lambda)$ is the photodiode responsivity and K is the conversion factor of the photodiode amplifier. Considering the beam geometry in Figure 2, the beam parameters can be related as

$$d_i = v * t_i = d_3 - 2x_i \tag{6}$$

In Eq. (6), v is the average velocity of the particle and t_i is the time of flight of a particle passing through any x_i position in the beam.

We need the peak-scattered intensity for a given velocity and time of flight, and the peak-scattered intensity can be either on the x axis or on the y axis depending on the orientation of the sensor and the direction of motion of the particles, i.e., vertical or horizontal. If we assume the particles are dropped vertically through the sensing volume, the y component of r in Eq. (2) would be zero. Thus, only the x component of r can play a role in that equation. Solving Eq. (6) for x_i, and substituting it for r into Eq. (4), Eq. (7) can be obtained.

$$P_{scat} = I_0\, e^{\left(-(d_3 - vt_i)^2 /_{2w^2}\right)}\, {}^{dC}\!/_{d\Omega}\, \Omega_c \tag{7}$$

Actual differential scattering cross-sections for each particle diameter and four different refractive indices were obtained using an online program [14]. Using actual values of $dC/d\Omega$, an equation was fitted to relate $dC/d\Omega$ to particle diameter [13].

$${}^{dC}\!/_{d\Omega} = 0.18d^2 \tag{8}$$

Combining Eqs. (3), (5), (7), and (8), we get

$$d(t_i,\, v, V_i,\, \Omega) = \left\{ \frac{2.78 * 10^6\, \pi w^2 V_i}{P_{tot} R(\lambda) K} Exp\left[\frac{(d_3 - vt_i)^2}{2w^2}\right] \frac{\Omega_i}{\Omega_c^2} \right\}^{0.5} \tag{9}$$

Eq. (9) can be used to determine the diameter of the particle. In this equation, Ω_c and Ω_i are the solid angles the photodiode makes with the center "c" of the beam and any x_i position in the beam, respectively.

4. RESULTS AND DISCUSSION

The mathematical model, i.e. Eq. (9), determines the particle diameter independent of the refractive index. This means that at 37±5° scattering angle, particulate matter of any type and material can be sized. To distinguish the type and material of the particle being detected by the photodiode, it is important to determine its refractive index. This can be done by measuring the scattered light intensity of the particle passing through the beam at a second scattering angle simultaneously. We have proposed the second scattering angle to be 90°. The scattered light measured at 90° can be used to develop another mathematical model which can be dependent on both size and refractive index. Hence, using the first model and the second model, particle diameter and refractive index can be determined simultaneously.

Since the refractive indices of the expected particles to be present in bleed air are known ahead of time; for example, refractive indices of water, benzene, diesel soot, propane soot, and engine oil are, 1.33, 1.4769, 1.8537, 1.7766, and 1.505 respectively, once our device determines the refractive index, the aerosol compound in bleed air can be retrieved accordingly.

As part of our future research plan, we will develop the second model for the 90° scattering angle. Although measuring the scattered light intensity at two angles is good enough to determine the particulate matter size and compound in bleed air, we are still interested to consider a third angle measurement so that we can determine the imaginary part of the refractive index as well.

As we can see in Figure 3, the independence of the differential scattering cross-section to the real part of the refractive index at 37° scattering angle gets weaker as the particle size is smaller than 10 µm. This research will be further extended to take the smaller particles into consideration as well.

5. Conclusion

We have proposed a novel technique using light scattering technology to distinguish between contaminant types in bleed air. This technique uses size and index of refraction as the measure. A mathematical model has been developed to determine the particle size independent of refractive index at 37° scattering angle. In addition to the 37°, we proposed that the scattered light intensity be measured at 90° angle to depend on both size and refractive index, and then the size and refractive index can be determined simultaneously.

ACKNOWLEDGEMENTS

Christopher M. Sorensen was supported by NSF Grant AGS-1649738.

REFERENCES

[1] Mann, G.W., S.J. Eckels, and B. W. Jones, *Analysis of particulate size distribution and concentrations from simulated jet engine bleed air incidents.* HVAC&R Research, 2014. **20**(7): p. 780-789.

[2] Winder, C. and J. Balouet, *Aircrew Exposure to Chemicals in Aircraft: Symptoms of Irritation and Toxicity*. Vol. 17. 2001.

[3] Byron W. Jones, S.N.A., Jake W. Roth, Mohammad H. Hosni, *The Nature of Particulates in Aircraft Bleed Air Resulting from Oil Contamination* in *ASHRAE Winter Conference*. 2017.

[4] Eckels, S.J., et al., *Aircraft Recirculation Filter for Air-Quality and Incident Assessment.* Journal of Aircraft, 2014. **51**(1): p. 320-326.

[5] van Netten, C., *Aircraft Air Quality Incidents, Symptoms, Exposures and Possible Solutions*, in *Air Quality in Airplane Cabins and Similar Enclosed Spaces*, M. Hocking, Editor. 2005, Springer Berlin Heidelberg: Berlin, Heidelberg. p. 193-210.

[6] Winder, C. and J. Balouet, *The Toxicity of Commercial Jet Oils*. Vol. 89. 2002. 146-64.

[7] Bartl, P., C. Völkl, and M. Kaiser, *Chemical characterization of polyol ester aviation lubricant residues.* Journal of Synthetic Lubrication, 2008. **25**(1): p. 1-16.

[8] van Netten, C., *Multi-elemental analysis of jet engine lubricating oils and hydraulic fluids and their implication in aircraft air quality incidents.* Sci Total Environ, 1999. **229**(1-2): p. 125-9.

[9] van Netten, C. and V. Leung, *Comparison of the constituents of two jet engine lubricating oils and their volatile pyrolytic degradation products.* Appl Occup Environ Hyg, 2000. **15**(3): p. 277-83.

[10] van Netten, C. and V. Leung, *Hydraulic fluids and jet engine oil: pyrolysis and aircraft air quality.* Arch Environ Health, 2001. **56**(2): p. 181-6.

[11] Eidhammer, T., D.C. Montague, and T. Deshler, *Determination of index of refraction and size of supermicrometer particles from light scattering measurements at two angles.* Journal of Geophysical Research: Atmospheres, 2008. **113**(D16): p. n/a-n/a.

[12] Hu, H., et al., *Determination of the refractive index and size distribution of aerosol from dual-scattering-angle optical particle counter measurements.* Applied Optics, 2006. **45**(16): p. 3864-3870.

[13] Waez, M.S., S.J. Eckels, and C.M. Sorensen, *A refractive-index and position-independent single-particle detector for large, nonabsorbing, spherical particles.* Aerosol Science and Technology, 2018: p. 1-8.

[14] Laven, P., *Separating diffraction from scattering: The million-dollar challenge*. Vol. 4. 2010.

